

Analyses of the Dispersion Overshoot and Inverse Dissipation of the High-Order Finite Difference Scheme

Qin Li^{1,2,*}, Qilong Guo¹ and Hanxin Zhang^{1,2}

¹ State Key Laboratory of Aerodynamics, Mianyang 621000, Sichuan, China

² National Laboratory of Computational Fluid Dynamics, Beijing University of Aeronautics and Astronautics, Beijing 100191, China

Received 25 October 2012; Accepted (in revised version) 18 April 2013

Available online 6 September 2013

Abstract. Analyses were performed on the dispersion overshoot and inverse dissipation of the high-order finite difference scheme using Fourier and precision analysis. Schemes under discussion included the pointwise- and staggered-grid type, and were presented in weighted form using candidate schemes with third-order accuracy and three-point stencil. All of these were commonly used in the construction of difference schemes. Criteria for the dispersion overshoot were presented and their critical states were discussed. Two kinds of instabilities were studied due to inverse dissipation, especially those that occur at lower wave numbers. Criteria for the occurrence were presented and the relationship of the two instabilities was discussed. Comparisons were made between the analytical results and the dispersion/dissipation relations by Fourier transformation of typical schemes. As an example, an application of the criteria was given for the remedy of inverse dissipation in Weirs & Martín's third-order scheme.

AMS subject classifications: 76M20, 74P99

Key words: High-order difference scheme, dispersion overshoot, inverse dissipation.

1 Introduction

High-order schemes are widely used in direct numerical simulation and large eddy simulation to resolve turbulent structures with broad length scales. Numerical simulation of shock/turbulent boundary layer interaction is an example that requires high order accuracy for capturing the broad length scales and the capability of shock capturing. The main advantage of the high-order scheme is the lower truncation error, which is obtained

*Corresponding author.

Email: qin-li@vip.tom.com (Q. Li)

through precision analyses. As shown in [1], the spectral characteristic of the scheme is another important attribute. It is not unusual that relative low-order schemes can have better dispersion/dissipation relation than that of higher-order ones.

Bandwidth optimization refers to the technique for improving the dispersion and/or dissipation features of difference schemes, which are derived through Fourier analysis. The methodology is to sacrifice the order of the scheme and use the available free parameters for optimization. Lele [2] and Tam [3] pioneered studies in this aspect from different considerations. Several variants of Tam's methods were proposed subsequently [4–6].

The optimization of the dispersion relation is to make the real part of the modified wave number ($\Re(\kappa')$) to distribute as close as possible along the theoretical one (κ). Generally, the dispersion curve of the standard center or upwinding-biased pointwise scheme moves below the theoretical straight line and drops to zero at π . Optimization tries to push the deviation of the curve to the line toward the higher band of the scaled wave number. Lockard [4] stressed that the moving of the curve above the theoretical one might happen in this process ("a noticeable overshoot"), which is called as dispersion overshoot in the paper. Because dispersion overshoot implies the possibility of excessive "deviation from the correct result for smaller values" (i.e., scaled wave numbers) like that in "Tam's operators" [4], which might result in phase errors for wave propagation, it is natural that attempts be made to solve the problem. A modified objective function was given by Lockard [4] to try to alleviate the phenomenon, but no analysis was given regarding the cause of the overshoot.

The numerical dissipation is another issue concerned by the optimization of upwinding-biased schemes. Usually some dissipation is necessary for numerical stability, especially in the case of shock capturing. As proposed by Adams & Shariff [5], the stability criterion is that, the imaginary part of the modified wave number satisfies: $\Im(\kappa') \leq 0$. This criterion has often been used by simply checking or requiring that the dissipation at π (called as $\pi_{dissipation}$ in the paper) be less than zero, and assuming that the criterion is satisfied in the region $[0, \pi]$ also. No further attempt is made to thoroughly check if the criterion is satisfied throughout the region.

To test Lockard's method, we used it to perform optimizations and obtained a third-order scheme (referred as LKD3), which used the same candidate schemes as that of the fifth-order WENO scheme but had different weights. The result showed that the optimized scheme still had minor dispersion overshoot, which indicated that the optimization method proposed by Lockard [4] might not truly solve the problem. In the meanwhile, when we checked the dissipation curve of Weirs & Martín's third-order scheme [6, 7] (referred as WM3), we found that the inverse dissipation existed at lower wave numbers. To explore above issues, we analyzed the dispersion overshoot and the inverse dissipation, and found the cause and criteria for the occurrence. The purpose of this study is not to develop a specific scheme, but to provide useful theoretical references to support bandwidth optimization of high-order schemes.

The paper is organized as follows. In Section 2, we report our investigations in pointwise high-order finite difference schemes, and present the analytical results; in Section 3,

we report the similar studies on schemes on staggered grids; and, in Section 4, we give concluding remarks.

2 Analyses of high-order finite difference pointwise schemes

The investigation is in the context of the one-dimensional hyperbolic conservation law:

$$u_t + f(u)_x = 0. \tag{2.1}$$

The domain is discretized into $x_i = i\Delta x$, where Δx is the discretization interval. There are at least two ways to represent a linear scheme, i.e., the explicit form

$$(f_x)_j \approx \frac{1}{\Delta x} \sum_{l=-M}^N a_l f(x_j + l\Delta x) \tag{2.2}$$

and the conservative weighted form:

$$(f_x)_j \approx -\frac{\hat{f}_{j+1/2} - \hat{f}_{j-1/2}}{\Delta x}, \tag{2.3a}$$

$$\hat{f}_{j+1/2} = \sum_{k=0}^{r'} C_k^r q_k^r \tag{2.3b}$$

$$q_k^r = \sum_{l=0}^{r-1} a_{k,l}^r f(u_{j-r+k+l+1}). \tag{2.3c}$$

The latter is constructed by the combination of the weighted candidate schemes, where r is the number of grid points in each grid stencil, r' is the number of stencils, $a_{k,l}^r$ is the coefficient of each candidate scheme, and C_k^r is the weight. A sketch for the most frequently-used WENO-like schemes on three-point stencils, the sketch is given in Fig. 1 for illustration. If the stencil represented by S_3 is included or $r' = r$, the stencils are symmetric; otherwise they are upwinding-biased or $r' = r - 1$.

It is easy to derive the formula of the modified scaled wave number of the scheme by Fourier transformation as [1-3]

$$\kappa' = \frac{-i}{\Delta x} \sum_{l=-M}^N a_l e^{il\kappa}, \tag{2.4}$$

where κ is the scaled wave number defined as $\kappa = k\Delta x$, and k is the wave number in Fourier transformation.

In the following, we investigate schemes when $r = 3$ in which the accuracy order of each candidate scheme is three and $a_{k,l}^r$ can be found in [8, 9]. For completeness, typical values for C_k^r are given in Table 1 according to final order R of the weighted scheme.

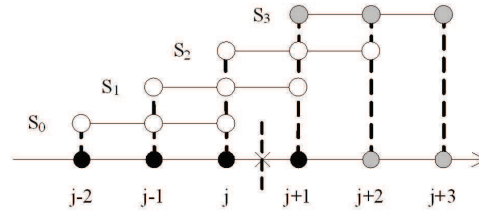


Figure 1: The schematic of candidate schemes on three-point stencils.

Several typical schemes can be expressed using Eqs. (2.3a)-(2.3c) and are also included in Table 1. Among them, the third-order schemes are like the linear WENO scheme (WENO3) with $R=3$, $C_2^3=C_3^3=0$ and $C_1^3=1$; Weirs & Martín’s optimized scheme (WM3) [6, 7]; and the optimized scheme using Lockard’s method [4] (LKD3), in which the objective function of optimization is

$$I = \int_0^{\kappa_1} \{ \sigma \text{Re}(\kappa' - \kappa)^2 + (1 - \sigma) [\text{Im}(\kappa') - \gamma \sin^\mu(\kappa/2)]^2 \} d\kappa$$

and the control parameters are ($\kappa_1=2\pi/7$, $\gamma=-13/32$, $\sigma=1/5$, $\mu=8$) [4]. Further, fourth-order schemes are like the center scheme with $R=4$ and $C_3^3=C_0^3=0$ and the Dispersion-Relation-Preservation scheme (DRP4) by Tam [3]. The fifth-order scheme is like the linear WENO scheme (WENO5) with $R=5$ and $C_3^3=0$. Finally, the sixth-order scheme is like the center scheme with $R=6$. In the paper, we abbreviate the scheme on upwinding-biased stencils ($C_3^3=0$) as the *UPW*-scheme, and the one on symmetric stencils ($C_3^3 \neq 0$) as the *SYM*-scheme.

Table 1: Weights C_k^3 for difference schemes.

R	$k=0$	$k=1$	$k=2$	$k=3$
3	$1 - C_1^3 - C_2^3 - C_3^3$	C_1^3	C_2^3	C_3^3
3(WM3)	0.094647545896	0.428074212384	0.408289331408	0.068988910312
3(LKD3)	0.113263320922852	0.546957397460938	0.339779281616211	0
4	C_0^3	$C_0^3 - 2C_3^3 + 1/2$	$-2C_0^3 + C_3^3 + 1/2$	C_3^3
4(DRP4)	0.07955985	0.42044007	0.42044007	0.07955985
5	$-C_3^3 + 1/10$	$-3C_3^3 + 3/5$	$3C_3^3 + 3/10$	C_3^3
6	$1/20$	$9/20$	$9/20$	$1/20$

2.1 Analyses of the dispersion overshoot

After careful checks on the dispersion curve of a scheme, it is found that the overshoot happens just after $\kappa=0$. This hints that the behavior of the following term

$$\frac{\Re(\kappa')}{\kappa} - 1 \tag{2.5}$$

Table 2: Dispersion relations of the UPW- and SYM-schemes.

R	$\Re(\kappa')$
3, 4	$\frac{\sin\kappa}{3} [4\tilde{C}_R \cos^2\kappa - (8\tilde{C}_R + 1)\cos\kappa + 4\tilde{C}_R + 4]$
5, 6	$\frac{\sin\kappa}{15} [2\cos^2\kappa - 9\cos\kappa + 22]$

Table 3: $\frac{\partial^{(i)}}{\partial\kappa^{(i)}}(\Re(\kappa')/\kappa - 1)(0)$ and overshoot criteria for weighted difference schemes.

R	$i=4$	$i=6$	Overshoot criterion
3, 4	$-4/5 + 8\tilde{C}_R$	$20/7 - 80\tilde{C}_R$	$\tilde{C}_R > 1/10$
5, 6	0	$-36/7$	N/A

should be studied at $\kappa = 0$. For completeness, the values of $\Re(\kappa')$ corresponding to Table 1 are given in Table 2.

In Table 2, $\tilde{C}_3 = 1 - C_1^3 - C_2^3$ and $\tilde{C}_4 = C_0^3 + C_3^3$. For the UPW-scheme, the highest order is five. After deriving derivatives of Eq. (2.5), we find that $\kappa = 0$ is a zero-value point of high order, i.e.,

$$\frac{\partial^{(i)}}{\partial\kappa^{(i)}}\left(\frac{\Re(\kappa')}{\kappa} - 1\right)(0) = 0,$$

for $i = 0, \dots, 3$ and 5. The details are shown in Table 3.

It is easy to derive the criterion for the occurrence of overshoot by requiring the first non-zero derivative be greater than zero, which are also included in Table 3. Using the criterion, checks can be made on the optimized schemes listed in Table 1. It is easy to see that WM3, LKD3 and DRP4 satisfy the conditions in Table 3 and overshoots occur. Among the schemes having overshoots, \tilde{C}_3 in LKD3 is the closest to 0.1 and produces the least overshoot. Fig. 2 gives the numerical relative error of the dispersion relation of typical schemes. The inset in the figure is an enlargement showing the overshoot of LKD3 which may be obscured in the main figure. Consistency is shown by the figure between numerical results and analytical results.

Based on the analytic relation in Table 3, we have the following observations:

1. When the critical state ($\tilde{C}_R = 1/10$) is met at $R = 3$, the dispersion relation turns out to be that of the fifth-order scheme, i.e.,

$$\frac{\sin\kappa}{15} [2\cos^2\kappa - 9\cos\kappa + 22],$$

with no overshoot.

2. Because

$$d(d^{(4)}(\Re(\kappa')/\kappa - 1)/d\kappa^4|_{\kappa=0})/d\tilde{C}_R = 8 = const$$

at $R = 3$ and 4, any "improvement" of the dispersion relation by optimization than that of the fifth-order scheme will cause dispersion overshoot, no matter what methods are used. And there is no possibility to further improve the dispersion

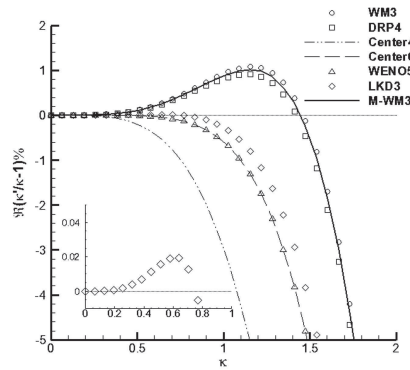


Figure 2: The relative error of dispersion of difference schemes.

relation of a fifth-order scheme due to the dispersion relation shown in Table 2 at $R=5,6$. In other words, the fifth-order scheme is at a special position which can not be surpassed if the non overshoot constraint is required.

3. The dispersion relation at $R=3$ is actually the same as that at $R=4$, which indicates that the third order optimized scheme theoretically can not further improve the relation than that of the fourth-order one. Similar idea and analyses can be used for the scheme whose candidate grid stencils have more than three points.

2.2 Analyses on inverse dissipation

In order to investigate the inverse dissipation phenomenon, we first deduce the dissipation relation ($\mathfrak{S}(\kappa')$) of the weighted difference scheme at different R . Based on $\mathfrak{S}(\kappa')$, $\pi_{dissipation}$ and the corresponding stability condition are obtained and shown in Table 4.

Similar to the development in the previous section, we investigate the inverse dissipation at the lower band of wave numbers by checking the behavior of ($\mathfrak{S}(\kappa')$) at $\kappa=0$, and find that $\kappa=0$ is a zero-value point of high order, i.e.,

$$\frac{\partial^{(i)}\mathfrak{S}(\kappa')}{\partial\kappa^{(i)}}(0) = 0$$

for $i=0, \dots, 3$ and 5. The details are tabulated in Table 5.

Comparing Tables 4 and 5, we find that, the stability based on $\pi_{dissipation}$ at $R=3$ can not guarantee that the scheme is stable at the lower wave number. For example, Table 1 shows that, for WM3, $2C_1^3+C_2^3+3C_3^3 = 1.471404487112 < 3/2$, which demonstrates the existence of inverse dissipation and the potential risk of instability; for LKD3, $2C_1^3+C_2^3+3C_3^3 = 1.433694076538087 < 3/2$, which also shows the same problem. However, for WENO3 and WENO5, two stability criteria are satisfied. As an example of the application of analytic results, we incorporated the criterion in Table 5 at $R=3$ into the optimization of WM3-like scheme, and obtained a modified solution (M-WM3) as $(C_0^3, C_1^3, C_2^3, C_3^3) =$

Table 4: Dissipation relations, $\pi_{dissipation}$ and corresponding stability criteria.

R	$\Im(\kappa')$	$\pi_{dissipation}$	Stability criterion
3	$\frac{1}{3}[(4-4C_1^3-4C_2^3-8C_3^3)\cos^3\kappa+(-9+8C_1^3+10C_2^3+18C_3^3)\cos^2\kappa+(6-4C_1^3-8C_2^3-12C_3^3)\cos\kappa+2C_2^3+2C_3^3-1]$	$\frac{1}{3}(-20+16C_1^3+24C_2^3+40C_3^3)$	$4C_1^3+6C_2^3\leq 5-10C_3^3$
4	$\frac{4}{3}(C_0^3-C_3^3)\cos^3\kappa-4(C_0^3-C_3^3)\cos^2\kappa+4(C_0^3-C_3^3)\cos\kappa-\frac{4}{3}(C_0^3-C_3^3)$	$-\frac{32}{3}(C_0^3-C_3^3)$	$C_0^3\geq C_3^3$
5	$\frac{2}{15}(1-20C_3^3)\cos^3\kappa-\frac{2}{3}(1-20C_3^3)\cos^2\kappa+\frac{2}{3}(1-20C_3^3)\cos\kappa-\frac{2}{15}(1-20C_3^3)$	$-\frac{16}{15}(1-20C_3^3)$	$C_3^3\leq 1/20$

Table 5: $\frac{\partial^{(i)}\Im(\kappa')}{\partial\kappa^{(i)}}(0)$ and corresponding stability criteria.

R	$i=4$	$i=6$	Stability criterion
3	$6-8C_1^3-4C_2^3-12C_3^3$	$-150+160C_1^3+140C_2^3+300C_3^3$	$2C_1^3+C_2^3\geq 3/2-3C_3^3$
4	0	$-120C_0^3+120C_3^3$	$C_0^3\geq C_3^3$
5	0	$-12+240C_3^3$	$C_3^3\leq 1/20$

(0.0902000403417333, 0.446821215154559, 0.39128933190972, 0.0716894125939877). M-WM3 has almost the same dispersion and dissipation relation as WM3 but satisfies the stability criterion. The numerical results are shown in Fig. 3.

Based on Tables 4 and 5, it is shown that two kinds of stability discussed above are equivalent at $R=4$ and $R=5$ but are different at $R=3$.

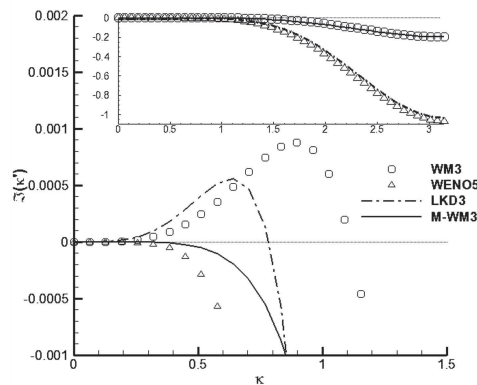


Figure 3: The dissipation of difference schemes at the lower band of wave numbers.

3 Analyses on high-order finite difference schemes on staggered grids

In [2], Lele proposed a class of center-type compact schemes on cell-centered meshes. What is more, the explicit finite difference scheme can be obtained in this class of compact schemes by simply setting $\alpha = \beta = 0$ in Eq. (B.1.1) in [2]. The obtained scheme can be thought as center schemes on staggered grids, and to fulfill the computation, interpolation schemes must be used to give the value at staggered grids. Theoretically, the

dispersion relation of the difference scheme will have a value close to π at $\kappa = \pi$, but it is a misunderstanding that such a scheme can fundamentally improve the dispersion relation because, when the interpolation is imbedded into the scheme, the dispersion curve of the combined scheme will still drop to zero. Also worth noting is that the optimization methods used in pointwise schemes in Section 2 can also be used in schemes on staggered grids. Similar analyses can be conducted except that two kinds of schemes will be involved, namely, the finite difference scheme and the interpolation scheme.

3.1 Analyses on the finite difference scheme

As in Section 2, the difference scheme for the spatial derivative of Eq. (2.1) can also be formulated in explicit form

$$(f_x)_j \approx \frac{1}{\Delta x} \sum_{l=-M}^N a_l f\left(x_j + \left(l + \frac{1}{2}\right)\Delta x\right) \tag{3.1}$$

and the conservative weighted form as Eq. (2.3a), where $\hat{f}_{j+1/2}$ and q_k^r are re-defined as:

$$\hat{f}_{j+1/2} = \sum_{k=k_0}^{r'} C_k^r q_k^r \tag{3.2a}$$

$$q_k^r = \sum_{l=0}^{r-1} a_{k,l}^r f(u_{j-r+k+l+1/2}). \tag{3.2b}$$

In this paper, the investigation is performed on the difference scheme on three-point stencil, which is sketched by Fig. 4. If the scheme uses stencils S_0 to S_2 (or $k_0 = 0$ and $r' = r - 1$ in Eq. (3.2a)), the scheme is upwinding-biased and called as the *UPW*-scheme as before. Otherwise it is symmetric and called as the *SYM*-scheme with $k_0 = 1$ and $r' = r$.

The modified wave number of the scheme has the form

$$\kappa' = -i \sum_{l=-M}^N a_l e^{i(l+1/2)\kappa}. \tag{3.3}$$

For completeness, the coefficients for $a_{k,l}^r$ in Eq. (3.2b) are tabulated in Table 6.

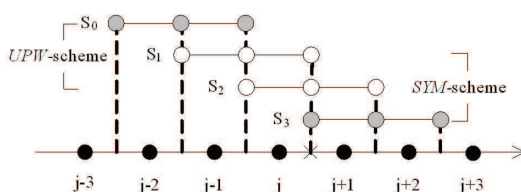


Figure 4: The schematic of three-point stencil and stencils on staggered grids.

Table 6: Coefficients $a_{k,l}^r$ for candidate difference schemes.

k	$l=0$	$l=1$	$l=2$
0	23/24	-35/12	71/24
1	-1/24	1/12	23/24
2	-1/24	13/12	-1/24
3	23/24	1/12	-1/24

Table 7: Weights C_k^3 for UPW-schemes.

R	$k=0$	$k=1$	$k=2$
3	C_0^3	C_1^3	$1 - C_0^3 - C_1^3$
4	C_0^3	$22C_0^3$	$-23C_0^3 + 1$
5	9/1840	99/920	71/80

Table 8: Weights C_k^3 for SYM-schemes.

R	$k=1$	$k=2$	$k=3$
3	C_1^3	C_2^3	$1 - C_1^3 - C_2^3$
4	C_1^3	$-2C_1^3 + 1$	C_1^3
6	-9/80	49/40	-9/80

The weights for the UPW-schemes are tabulated in Table 7, and those for the SYM-schemes are tabulated in Table 8.

The coefficients for SYM-schemes at the sixth-order in Table 8 are actually implicitly included in the scheme by Lele [2].

3.1.1 Analyses of the dispersion overshoot

Following the similar idea in Section 2.1, we derive the derivatives of Eq. (2.5) up to sixth order. It is also found that $\kappa=0$ is a zero-value point of high order, i.e.,

$$\frac{\partial^{(i)}}{\partial \kappa^{(i)}} (\Re(\kappa') / \kappa - 1)(0) = 0$$

for $i=0, \dots, 3$ and 5. The non-zero derivatives are tabulated in Table 8.

Based on Table 9 and the dispersion relation not shown in the paper, we give the following remarks:

1. For the UPW-scheme at $R=3$ in Tables 7 and 9, when the critical state ($68C_0^3 - C_1^3 = 9/40$) occurs and $C_0^3 = 9/1840$, it is easy to check that the scheme actually turns into a fifth-order scheme. Under the critical state, it can also be found that, when $0 < C_0^3 < 9/1840$, the dispersion relation can be slightly improved than that of the fifth-order scheme, and the best one can be obtained by setting $C_0^3=0$; when $C_0^3 \leq 149/3680$, $\kappa'(\pi)$ will have a positive value.

- For the UPW-scheme at $R=4$ in Tables 7 and 9, when $C_0^3=9/1840$, the scheme will upgrade to the fifth-order one without overshoot. Since

$$d(d^{(4)}(\Re(\kappa')/\kappa-1)/d\kappa^4|_{\kappa=0})/dC_0^3=23=const$$

any optimization to the fourth-order scheme will cause overshoot. It can also be found that, in order to yield a scheme with convex coefficients, C_0^3 should be less or equal than $1/22$, and $\kappa'(\pi)|_{C_0^3=1/22}=31/33$.

- For the SYM-scheme, dispersion relations of the third and fourth order are the same, which implies the third-order optimized scheme theoretically can not further improve the relation than that of the fourth-order one.
- For the SYM-scheme at $R=4$ in Tables 8 and 9, when the critical state ($C_2^3=49/40$) happens, the scheme will upgrade to sixth order without overshoot. Because

$$d(d^{(4)}(\Re(\kappa')/\kappa-1)/d\kappa^4|_{\kappa=0})/dC_2^3=1/2=const$$

at $R=3$ and 4 , any attempts to improve the dispersion relation of the third- or fourth-scheme will cause overshoot. So the dispersion relation of the sixth-order scheme is at a special position which can not be further improved if the non overshoot constraint is imposed. Particularly, the weights of the sixth-order scheme are observed to be a non-convex combination because $C_1^3=C_3^3 < 0$.

Table 9: $\frac{\partial^{(i)}}{\partial \kappa^{(i)}}(\Re(\kappa')/\kappa-1)(0)$ and overshoot criteria for UPW- and SYM-schemes.

R		$i=4$	$i=6$	Overshoot criterion
The UPW-Scheme	3	$-\frac{9}{80}+34C_0^3-\frac{1}{2}C_1^3$	$\frac{45}{224}-\frac{1115}{2}C_0^3+\frac{25}{8}C_1^3$	$68C_0^3-C_1^3 > \frac{9}{40}$
	4	$-\frac{9}{80}+23C_0^3$	$\frac{45}{224}-\frac{1955}{4}C_0^3$	$C_0^3 > \frac{9}{1840}$
	5	0	$-\frac{981}{448}$	N/A
The SYM-Scheme	3, 4	$-\frac{49}{80}+\frac{1}{2}C_2^3$	$\frac{745}{224}-\frac{25}{8}C_2^3$	$C_2^3 > \frac{49}{40}$
	5	N/A	N/A	N/A
	6	0	$-\frac{225}{448}$	N/A

3.1.2 Analyses on inverse dissipation

For schemes on staggered grids, it is easy to find by analytic relations of the dissipation that, all $\pi_{dissipation}$ equal to zero. After checking the behavior of $\Im(\kappa')$ at $\kappa=0$, it is also found that $\kappa=0$ is a zero-value point of high-order, i.e.,

$$\frac{\partial^{(i)}\Im(\kappa')}{\partial \kappa^{(i)}}(0)=0$$

for $i=0, \dots, 3$ and 5 . The details are shown in Table 10.

The corresponding stability criteria are also given in the table. From Tables 7, 8 and 10, we give the following remarks:

Table 10: $\frac{\partial^{(i)}\mathfrak{S}(\kappa')}{\partial\kappa^{(i)}}(0)$ and stability criteria for *UPW*- and *SYM*-schemes.

<i>R</i>		<i>i</i> = 4	<i>i</i> = 6	Stability criterion
The <i>UPW</i> -Scheme	3	$22C_0^3 - C_1^3$	$-\frac{1765}{2}C_0^3 + \frac{35}{4}C_1^3$	$C_0^3 \leq \frac{1}{22}C_1^3$
	4	0	$-690C_0^3$	$C_0^3 \geq 0$
	5	0	$-\frac{27}{8}$	N/A
The <i>SYM</i> -Scheme	3	$-2C_1^3 - C_2^3 + 1$	$\frac{35}{2}C_1^3 + \frac{35}{4}C_2^3 - \frac{35}{4}$	$2C_1^3 + C_2^3 \geq 1$
	4	0	0	N/A
	6	0	0	N/A

1. For the *UPW*-schemes, when $C_0^3 = C_1^3/22$ at $R = 3$, the scheme will upgrade to the fourth-order scheme, whose stability depends on the sign of C_0^3 . When $C_0^3 = 0$ at $R = 4$, the scheme will become the standard fourth-order center scheme with one staggered grid point vanishing.
2. For *SYM*-schemes, when $2C_1^3 + C_2^3 = 1$ at $R = 3$, the scheme will upgrade to the fourth-order center-type scheme without dissipation. Dissipative schemes can only occur for third-order cases.

3.2 Analyses on the interpolation scheme

In order to compute derivatives using the scheme defined on the staggered grids (see Eqs. (3.1)-(3.2b)), the interpolation is needed to give the value of the variables on staggered grids. Deng et al. first proposed an adaptive, ENO-like interpolation algorithm [10]. Later Deng constructed a weighted form of interpolation similar to WENO [11]. Deng et al.'s scheme is based on upwinding-biased stencils (referred as the *UPW*-scheme) which have three grid points. It appears natural to construct the symmetric form which includes the *UPW*-scheme. The complete form of the interpolation can be expressed as:

$$u_{i+1/2} = \sum_{k=0}^{r'} D_k^r p_k^r \tag{3.4a}$$

$$p_k^r = \sum_{l=0}^{r-1} b_{k,l}^r u_{i-r+1+k+l}, \tag{3.4b}$$

where p_k^r is the candidate interpolation scheme and r' is the number of stencils used. The scheme is upwinding-biased if $r' = r - 1$ (the *UPW*-scheme) and symmetric if $r' = r$ (the *SYM*-scheme). A schematic for the commonly-used schemes on a three-point stencil is given by Fig. 5.

In the following, we investigate schemes when $r = 3$ in which the accuracy order of each candidate scheme is three. For completeness, the coefficients $b_{k,l}^r$ are given in Table

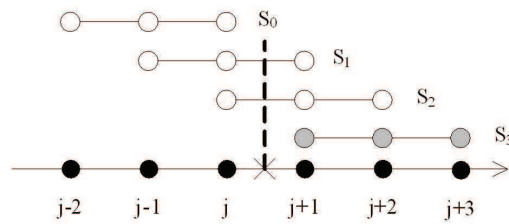


Figure 5: The schematic of interpolation schemes on three-point stencils.

Table 11: Coefficients $b_{k,l}^r$ for candidate interpolation schemes.

k	$l=0$	$l=1$	$l=2$
0	8/3	-5/4	15/8
1	-1/8	3/4	3/8
2	3/8	3/4	-1/8
3	15/8	-5/4	3/8

Table 12: Weights D_k^3 for interpolation schemes.

R	$k=0$	$k=1$	$k=2$	$k=3$
3	D_0^3	D_1^3	$1 - D_0^3 - D_1^3 - D_3^3$	D_3^3
4	D_0^3	$2D_0^3 - 3D_3^3 + 1/2$	$-3D_0^3 + 2D_3^3 + 1/2$	D_3^3
5	$1/16 - D_3^3$	$5/8 - 5D_3^3$	$5/16 + 5D_3^3$	D_3^3
6	1/32	15/32	15/32	1/32

11, while D_k^r is shown in Table 12 with respect to the final order R . Especially, D_k^r of the UPW-scheme can be explicitly obtained by setting $D_3^3 = 0$.

By substituting Eq. (3.4b) into Eq. (3.4a), we can derive the analytic forms of the modified wave number of the scheme at various R by Fourier analysis, and analyze the dispersion and dissipation relation of the scheme as before.

3.2.1 Analyses of the dispersion overshoot

For completeness, Table 13 shows the $\Re(\kappa')$ expressions of the interpolation schemes.

In Table 13, $\tilde{D}_0^3 = D_0^3 + D_3^3$. For the UPW-scheme the highest order is five. After checking

$$\frac{\partial^{(i)}}{\partial \kappa^{(i)}} (\Re(\kappa') / \kappa - 1)$$

at $\kappa = 0$, we also find that the value at this point vanishes with high order for $i = 0, \dots, 3$ and 5. The details and corresponding dispersion overshoot criteria are shown in Table 14.

For the UPW-scheme the highest order is also five. Based on the results in Tables 14 and 13, we give the following remarks:

Table 13: Dispersion relations of the UPW- and SYM-schemes.

R	$\Re(\kappa')$
3, 4	$\frac{\cos(\kappa/2)}{2} [12\tilde{D}_0^3 \cos^4(\kappa/2) - (24\tilde{D}_0^3 + 1) \cos^2(\kappa/2) + 12\tilde{D}_0^3 + 3]$
5, 6	$\frac{\cos(\kappa/2)}{8} [3 \cos^4(\kappa/2) - 10 \cos^2(\kappa/2) + 15]$

Table 14: $\frac{\partial^{(i)}}{\partial \kappa^{(i)}} (\Re(\kappa'/\kappa - 1))(0)$ and overshoot criteria for weighted interpolation schemes.

R	$i = 4$	$i = 6$	Dispersion criterion
3, 4	$-\frac{9}{16} + 9\tilde{D}_0^3$	$\frac{45}{32} - \frac{315}{4}\tilde{D}_0^3$	$\tilde{D}_0^3 > \frac{1}{16}$
5, 6	0	$-\frac{225}{64}$	N/A

1. When the critical state occurs at $R=3$ and 4, i.e., $\tilde{D}_0^3 = 1/16$, the dispersion relation is the same as that at $R=5$ and 6, where there is no overshoot; The order of the scheme at $R=4$ will increase by at least one order, and a further increase may be possible depending on the choice of the rest free parameter of D_k^r .

2. Because

$$d(d^{(4)}(\Re(\kappa')/\kappa - 1)/d\kappa^4|_{\kappa=0})/d\tilde{D}_0^3 = 9 = const$$

any "improvement" of the dispersion relation by optimization with respect to that of the fifth- or sixth-order scheme will cause overshoot.

3. Because the dispersion relation of the fifth-order scheme is the same as that of sixth-order, there is of no possibility for further optimization on the dispersion relation, but there is availability to adjust the dissipation of the scheme to a desired level, which can be seen in Table 15 at $R=5$ in Section 3.2.2.
4. Because the dispersion relation of the third-order scheme is the same as that of fourth order, it is not necessary to develop any third-order optimized scheme, which can not further improve the dispersion relation but is one order lower than the fourth-order counterpart.

3.2.2 Analyses on inverse dissipation

In a similar way, we first study the stability problem at π . The dissipation relation ($\Im(\kappa')$) of the interpolation schemes can be deduced and $\pi_{dissipation}$ can be computed. Expressions for $\Im(\kappa')$, $\pi_{dissipation}$ and corresponding stability condition are tabulated in Table 15.

Then we check the behavior of $\Im(\kappa')$ at $\kappa = 0$, and find that $\kappa = 0$ is also a zero-value point of high order, i.e.,

$$\frac{\partial^{(i)} \Im(\kappa')}{\partial \kappa^{(i)}}(0) = 0$$

for $i = 0, \dots, 3$ and 5. The details are shown in Table 16.

Based on the results in Tables 15 and 16, we give the following remarks:

Table 15: Dissipation relations, $\pi_{dissipation}$ and corresponding stability criteria.

R	$\Im(\kappa')$	$\pi_{dissipation}$	Stability criterion
3	$\frac{1}{2}\sin^3(\kappa/2) [12(D_0^3 - D_3^3)\cos^2(\kappa/2) - 8D_0^3 - 2D_1^3 + 6D_3^3 + 1]$	$-4D_0^3 - D_1^3 + 2D_3^3 + 1/2$	$4D_0^3 + D_1^3 \geq 1/2 + 3D_3^3$
4	$-6\sin^5(\kappa/2)(D_0^3 - D_3^3)$	$-6D_0^3 + 6D_3^3$	$D_0^3 \geq D_3^3$
5	$-\frac{3}{8}\sin^5(\kappa/2)(1 - 32D_3^3)$	$-3/8 + 12D_3^3$	$D_3^3 \leq 1/32$
6	0	0	N/A

Table 16: $\frac{\partial^{(i)}\Im(\kappa')}{\partial\kappa^{(i)}}(0)$ and stability criteria.

R	$n=3$	$n=5$	Stability criterion
3	$\frac{3}{2}D_0^3 - \frac{3}{4}D_1^3 - \frac{9}{4}D_3^3 + \frac{3}{8}$	$-\frac{105}{4}D_0^3 + \frac{15}{8}D_1^3 + \frac{225}{8}D_3^3 - \frac{15}{16}$	$6D_0^3 - 3D_1^3 \geq 9D_3^3 - \frac{3}{2}$
4	0	$-\frac{45}{2}(D_0^3 - D_3^3)$	$D_0^3 \geq D_3^3$
5	0	$45D_3^3 - \frac{45}{32}$	$D_3^3 \leq 1/32$
6	0	0	N/A

1. When $D_0^3 = D_3^3$ happens at $R=4$, the scheme will become a center-type scheme, which includes the standard fourth order center scheme at $D_0^3 = D_3^3 = 0$.
2. When $D_3^3 = 1/32$ for SYM-scheme at $R=5$, the scheme will upgrade to the sixth order center scheme without dissipation.
3. For schemes at $R=4$ and 5, we can see that the stability criteria derived through inverse dissipation at $\kappa = \pi$ and 0 are the same, which indicates that the easily-realized stability at π can guarantee the stability at the lower wave number. But the situation differs at $R=3$: the inverse dissipation might happen at the lower band although the scheme is stable at $\kappa = \pi$.

4 Conclusions

We performed systematic investigations on the dispersion overshoot and inverse dissipation related to the high-order difference scheme. Inverse dissipation is discussed in two aspects: that at the scaled wave number π , and that at the lower wave number. The latter is not obvious and is usually ignored in pervious studies. The high-order schemes consist of two types: the first are the pointwise schemes, and the other are those constructed on staggered grids. For each type, two kinds of schemes were comparatively studied, namely, the UPW- and SYM-schemes. These discussed schemes, which are based on third-order candidate schemes on three-point stencils, cover commonly-used forms to some extent. Analyses were performed and a comprehensive theoretical reference was set up thereafter, which can be used as references for the bandwidth optimization.

Although the dispersion overshoot has been already reported by others, it is usually superficially studied. We present a theoretical foundation of the overshoot and the criteria for its occurrence. We point out that nearly all previous optimized schemes will

have inevitable overshoot after optimization if the purpose of the optimization is to get a improved dispersion relation than that at the critical state. The only exception lies in the third-order *UPW*-scheme on staggered grids. It appears impossible to develop a specific optimization method to eliminate the overshoot. The reasonable requirement for optimizations should be rather how much the overshoot can be tolerated. It was found that theoretical constraints exist in optimization, i.e., non further improvement can be obtained for third- or fifth-order scheme by degrading one order from the fourth- or sixth-counterparts respectively.

Two types of inverse dissipation have been discussed, especially that at the lower wave number. The theoretical foundation of this issue is investigated and the criteria for the occurrence of inverse dissipation are given. For pointwise and interpolation schemes discussed in the paper, it was found that two types of stability are equivalent for schemes of fourth and higher order, but they are different for the third-order schemes. The dissipation of the third-order scheme may have a stable negative value at $\kappa = \pi$ but be positive around $\kappa = 0$.

The results indicate that within schemes discussed in the paper, the third-order pointwise and interpolation optimized schemes can not further improve the dispersion relation than the fourth-order scheme but with a loss of one accurate order; what is more, there exists the risk of inverse dissipation if schemes are not carefully designed. So from our view, it is not suggested to construct third-order optimized schemes.

Tests on the available schemes show the agreement between the theoretical conclusions and numerical schemes. The outcomes of the analyses can serve as remedies for the scheme having inverse dissipation problem.

Acknowledgments

This work was sponsored by the National Science Foundation of China under Grant number 10972023 and 11272037, and also partially supported by National Basic Research Program of China (No. 2009CB724100). The first author was very grateful to Prof. Frank Lu for his efforts on the revision of the manuscript.

References

- [1] R. VICHNEVETSKY AND J. B. BOWLES, *Fourier Analysis of Numerical Approximations of Hyperbolic Equations*, SIAM, Philadelphia, 1982.
- [2] S. K. LELE, *Compact finite difference schemes with spectral-like resolution*, J. Comput. Phys., 103 (1992), pp. 16–42.
- [3] C. K. W. TAM AND J. C. WEBB, *Dispersion-relation-preserving finite difference schemes for computational acoustics*, J. Comput. Phys., 107 (1993), pp. 262–281.
- [4] D. P. LOCKARD, K. S. BRENTNER AND H. L. ATKINS, *High-accuracy algorithms for computational aeroacoustics*, AIAA J., 33 (1995), pp. 246–251.

- [5] N. A. ADAMS AND K. SHARIFF, *A high-resolution hybrid compact-ENO scheme for shock-turbulence interaction problems*, J. Comput. Phys., 127 (1996), pp. 27–51.
- [6] V. G. WEIRS AND G. V. CANDLER, *Optimization of weighted ENO schemes for DNS of compressible turbulence*, AIAA 97-1940, 1997.
- [7] M. P. MARTÍN, E. M. TAYLOR, M. WU AND V. G. WEIRS, *A bandwidth-optimized weno scheme for the direct numerical simulation of compressible turbulence*, J. Comput. Phys., 220 (2006), pp. 270–289.
- [8] C. W. SHU AND S. OSHER, *Efficient implementation of essentially non-oscillatory shock capturing schemes*, J. Comput. Phys., 77 (1988), pp. 439–471.
- [9] C. W. SHU, *Essentially non-oscillatory and weighted essentially, non-oscillatory schemes for hyperbolic, Conservation Laws*, NASA/CR-97-206253, ICASE Report No. 97-65.
- [10] X. G. DENG AND H. MAEKAWA, *Compact high-order accurate nonlinear schemes*, J. Comput. Phys., 130 (1997), pp. 77–91.
- [11] X. G. DENG AND H. X. ZHANG, *Developing high-order weighted compact nonlinear schemes*, J. Comput. Phys., 165 (2000), pp. 22–44.